

## Searches for heavy long-lived sleptons and $R$ -hadrons with the ATLAS detector

Sascha Mehlhase<sup>1,a</sup>, on behalf of the ATLAS Collaboration.

<sup>1</sup>Niels Bohr Institute, University of Copenhagen, Copenhagen, Denmark

**Abstract.** A search for long-lived particles is performed using a data sample of  $4.7 \text{ fb}^{-1}$  from proton-proton collisions at a centre-of-mass energy  $\sqrt{s} = 7 \text{ TeV}$  collected by the ATLAS detector at the LHC. No excess is observed above the estimated background and lower limits, at 95% confidence level, are set on the mass of the long-lived particles in different scenarios, based on their possible interactions in the inner detector, the calorimeters and the muon spectrometer. Long-lived staus in gauge-mediated SUSY-breaking models are excluded up to a mass of 300 GeV for  $\tan\beta = 5 - 20$ . Directly produced long-lived sleptons are excluded up to a mass of 278 GeV.  $R$ -hadrons, composites of gluino (stop, sbottom) and light quarks, are excluded up to a mass of 985 GeV (683 GeV, 612 GeV) when using a generic interaction model. Additionally two sets of limits on  $R$ -hadrons are obtained that are less sensitive to the interaction model for  $R$ -hadrons. One set of limits is obtained using only the inner detector and calorimeter observables, and a second set of limits is obtained based on the inner detector alone. The full paper can be found in [1].

### 1 Introduction

Heavy long-lived particles (LLP) are predicted in a range of theories which extend the Standard Model (SM). Supersymmetry (SUSY) [2–10] models allow long-lived sleptons, squarks and gluinos. The searches are optimised for the different experimental signatures of sleptons and composite colourless states of a squark or gluino together with SM quarks and gluons, called  $R$ -hadrons. The results of a search for long-lived sleptons, identified in both the inner detector (ID) and in the muon spectrometer (MS), (“slepton search”) are interpreted in the framework of gauge-mediated SUSY breaking (GMSB) [11–17] with the light stau as the LLP. Direct pair production of sleptons is also used to interpret the data independently of the mass spectrum of the other SUSY particles.  $R$ -hadrons may emerge as charged or neutral states from the  $pp$  collision and be converted to a state with a different charge by interactions with the detector material, and thus arrives as neutral, charged or doubly charged particles in the muon spectrometer. In ATLAS, LLPs can be identified via the timing information in the muon spectrometer or calorimeters, and via the measurement of the energy loss in the silicon pixel detector. These techniques are combined in this analysis to achieve optimal sensitivity for the “full-detector  $R$ -hadron search”. In addition searches based on only the calorimeter and pixel detector information (“MS-agnostic  $R$ -hadron search”), and based solely on the pixel detector (“ID-only  $R$ -hadron search”) are performed. The latter two cases are motivated by the limited understanding of  $R$ -hadron interactions in matter, in particular for possible electrically

neutral  $R$ -hadrons traversing the MS. Furthermore, these searches are sensitive to scenarios in which the  $R$ -hadrons decay before reaching the MS. In all searches the signal particles are assumed to be stable within the ATLAS detector, at least to the point they hit the last relevant component of the subdetector used for detecting it.

### 2 Data and simulated samples

The studies are based on  $4.7 \text{ fb}^{-1}$  of  $pp$  collision data collected at a centre-of-mass energy  $\sqrt{s} = 7 \text{ TeV}$  in 2011. The events are selected online by muon triggers for the slepton search and by missing transverse momentum and muon triggers for the  $R$ -hadron searches. Data and Monte Carlo simulation  $Z \rightarrow \mu\mu$  samples are used for timing resolution studies. Monte Carlo signal samples are used to study the expected signal behaviour and to set limits. The GMSB samples are generated with stau masses between 122.2 and 465 GeV. The  $R$ -hadron samples are generated with gluino masses ranging from 300 to 1500 GeV and squark masses between 200 and 1000 GeV.

### 3 The ATLAS detector

The ATLAS detector [18] is a multipurpose particle physics detector with a forward-backward symmetric cylindrical geometry and near  $4\pi$  coverage in solid angle. The ID consists of a silicon pixel detector, a silicon micro-strip detector, and a transition radiation tracker. The ID is surrounded by a thin superconducting solenoid providing a 2 T magnetic field, and by

<sup>a</sup>e-mail: sascha.mehlhase@nbi.dk

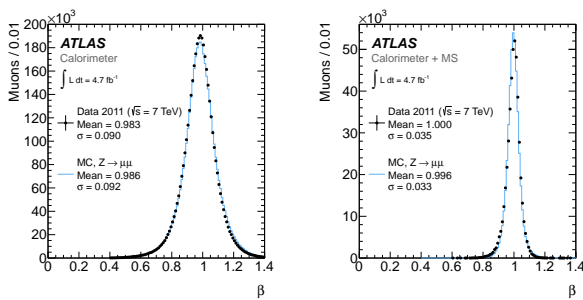


**Figure 1.** Distribution of  $\beta$  for selected  $Z \rightarrow \mu\mu$  decays in data and MC, for calorimeter (left) and combined (right) measurements. [1]

high-granularity liquid-argon sampling electromagnetic calorimeters (LAr). An iron/scintillator-tile calorimeter provides coverage for hadrons in the central rapidity range. The end-cap and forward regions are instrumented with liquid-argon calorimeters for both electromagnetic and hadronic measurements. The MS surrounds the calorimeters and consists of three large superconducting air-core toroids each with eight coils, a system of precision tracking chambers, and detectors for triggering.

The ATLAS trigger system is designed to select the events of interest with a data taking rate of about 400 Hz from a beam bunch crossing rate as high as 40 MHz.

The relation between the time-of-flight and the charge deposition in each pixel is measured in dedicated calibration scans and shows a good linearity. Therefore the time-of-flight measurement is well correlated with the energy loss  $dE/dx$  of a charged particle in the pixel detector. The masses of slow charged particles can be measured by fitting each  $dE/dx$  and momentum measurement to an empirical Bethe-Bloch function.

The ATLAS tile and LAr calorimeters have sufficiently good timing resolutions to distinguish highly relativistic SM particles from the slower moving LLPs. The time resolution depends on the energy deposited in the cell and also the layer type and thickness, but typical resolutions are 2 ns for an energy deposit of 1 GeV and generally better for the tile calorimeter.

The velocity  $\beta$  of a particle is estimated using two subsystems, the monitored drift tube chambers as well as the resistive plate chambers. For the former, individual track segments are reconstructed with different  $\beta$  values and an estimate is given by choosing those yielding the best match. In a successive track re-fit the  $\beta$  estimation is improved further. For the resistive plate chambers, a  $\beta$  estimate is obtained by averaging the  $\beta$ 's calculated separately from the time-of-flight associated to each hit.

Depending on the search strategy and in case the measurements are consistent and  $\beta > 0.2$ , a weighted average is obtained, using the calculated error of each measurement times the pull of the  $\beta$  distribution for muons from  $Z \rightarrow \mu\mu$  samples as weights.

## 4 LLP candidate and event selection

A common base selection, requiring a functional detector, a well reconstructed primary vertex and vetoing on cosmic muons is applied. Furthermore two dedicated LLP candidate and event selections are used for the two different signal types studied: sleptons and  $R$ -hadrons.

### 4.1 Sleptons

Candidate events are selected with a single muon trigger with about 85% efficiency. For two LLP candidate events a loose selection requires a transverse momentum above 50 GeV, an invariant mass outside the  $Z$  mass region ( $\pm 10$  GeV) and a combined  $\beta$  below 0.95. For one LLP candidate events a tight selection demands a transverse momentum above 70 GeV, a  $\beta$  consistent at  $2\sigma$  amongst at least two different sub-detectors. In both cases, a model dependent cut on the candidate mass  $m_\beta = p/\gamma\beta$  is applied. The typical overall signal selection efficiency is about 20%.

### 4.2 $R$ -hadrons

Candidate events are selected with a 60 – 70 GeV missing transverse momentum trigger with between 15 and 20% signal efficiency. In the full-detector and MS-agnostic search candidates are required to have a momentum above 140 GeV, be isolated from jets and other tracks, be in the central region and have a good combined or standalone calorimeter  $\beta$ . In addition  $\beta\gamma < 1.5 - 2.0$  and  $\beta < 0.8 - 0.9$  are required. The typical signal selection efficiency is around 10%. In the ID-only search candidates are required to have a momentum above 100 GeV, a transverse momentum above 50 GeV, even tighter isolation, an electron veto and a offline missing transverse energy above 85 GeV. In addition the  $dE/dx$  value has to exceed a pseudorapidity-dependent threshold.

## 5 Background estimation

The background for all searches is mostly composed of high- $p_T$  muons with mis-measured  $\beta$  or large ionisation. The background estimation is derived from data in all cases. The background mass spectrum (examples shown in Figure 2) is estimated by calculating a mass from the  $p_T$ -spectrum of candidates and the measured  $\beta$  distribution of the background obtained from control samples.

## 6 Systematic uncertainties

Signal cross sections are calculated to next-to-leading order in the strong coupling constant, adding the resummation of soft gluon emission at next-to-leading-logarithmic accuracy (NLO+NLL) [19–25]. This leads to 5% relative uncertainty on the expected signal normalisation in the slepton search, and 15 to 30% uncertainty for the  $R$ -hadron search. The uncertainty on the expected signal, taking into

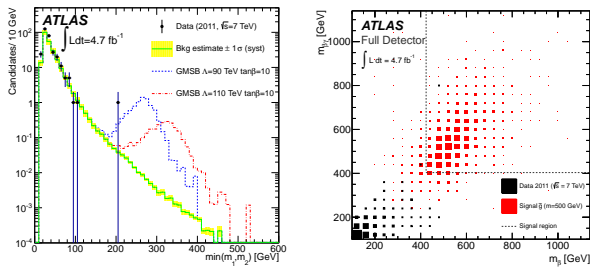


**Figure 2.** Observed data, background estimate and expected signal in the two-candidate signal region in the slepton search (left) and in the full-detector  $R$ -hadron search (right). [1]

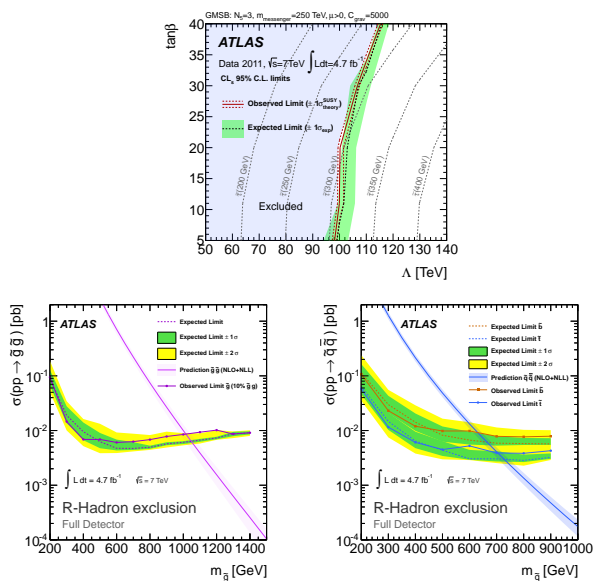


**Figure 3.** Limits on the SUSY-breaking mass scale,  $\Lambda$ , and the ratio of the vacuum expectation values of the two Higgs doublets,  $\tan\beta$ , in GMSB models (top), cross-section upper limits for gluino (bottom left) and squark (bottom right)  $R$ -hadrons in the full-detector search. [1]

account systematic discrepancies between data and simulation in trigger efficiency, momentum resolution,  $\beta$  and  $dE/dx$  calibrations, missing energy scale and QCD uncertainties is estimated to 4–6% for sleptons and 11–13% for  $R$ -hadrons. The uncertainty on the background estimate, taking into account variations of distributions and statistics, was found to be 11%/13% for the one/two-candidate slepton search and 15–20% for the  $R$ -hadron search. An uncertainty of 3.9% [26, 27] is assigned to the integrated luminosity corresponding to the dataset.

## 7 Results

No indication of signal above the expected background is observed. Upper cross-section limits on new particles are set by counting the number of events passing a set of mass

cuts optimised for each given mass point and model. For the ID-only analysis the full mass spectrum of the background and the hypothetical signal is considered. Cross-section limits are obtained using the  $CL_s$  method [28] and a 95% confidence level. Long-lived staus in the GMSB model considered, for  $\tan\beta = 5 - 20$ , are excluded at 95% CL for masses up to 300 GeV, while directly produced long-lived sleptons, or sleptons decaying to long-lived ones, are excluded at 95% CL up to a stau mass of 278 GeV for models with slepton mass splittings smaller than 50 GeV. Exemplary limit plots are shown in Figure 3.

## References

- [1] ATLAS Collab., CERN-PH-EP-2012-236 (2012)
- [2] H. Miyazawa, Prog. Theor. Phys. **36** (6), 1266 (1966)
- [3] P. Ramond, Phys. Rev. **D3**, 2415 (1971)
- [4] Y.A. Gol'fand, E.P. Likhman, JETP Lett. **13**, 323 (1971), [Pisma Zh.Eksp.Teor.Fiz.13:452-455,1971]
- [5] A. Neveu, J.H. Schwarz, Nucl. Phys. **B31**, 86 (1971)
- [6] A. Neveu, J.H. Schwarz, Phys. Rev. **D4**, 1109 (1971)
- [7] J. Gervais, B. Sakita, Nucl. Phys. **B34**, 632 (1971)
- [8] D.V. Volkov, V.P. Akulov, Phys. Lett. **B46**, 109 (1973)
- [9] J. Wess, B. Zumino, Phys. Lett. **B49**, 52 (1974)
- [10] J. Wess, B. Zumino, Nucl. Phys. **B70**, 39 (1974)
- [11] M. Dine, W. Fischler, Phys. Lett. **B110**, 227 (1982)
- [12] L. Alvarez-Gaume, M. Claudson, M.B. Wise, Nucl. Phys. **B207**, 96 (1982)
- [13] C.R. Nappi, B.A. Ovrut, Phys. Lett. **B113**, 175 (1982)
- [14] M. Dine, A.E. Nelson, Phys. Rev. **D48**, 1277 (1993)
- [15] M. Dine, A.E. Nelson, Y. Shirman, Phys. Rev. **D51**, 1362 (1995)
- [16] M. Dine, A.E. Nelson, Y. Nir, Y. Shirman, Phys. Rev. **D53**, 2658 (1996)
- [17] C.F. Kolda, Nucl. Phys. Proc. Suppl. **62**, 266 (1998)
- [18] ATLAS Collab., JINST **3**, S08003 (2008)
- [19] W. Beenakker, R. Hopker, M. Spira, P.M. Zerwas, Nucl. Phys. **B492**, 51 (1997)
- [20] W. Beenakker, M. Kramer, T. Plehn, M. Spira, P.M. Zerwas, Nucl. Phys. **B515**, 3 (1998)
- [21] A. Kulesza, L. Motyka, Phys. Rev. Lett. **102**, 111802 (2009)
- [22] A. Kulesza, L. Motyka, Phys. Rev. **D80**, 095004 (2009)
- [23] W. Beenakker, S. Brensing, M. Kramer, A. Kulesza, E. Laenen et al., JHEP **0912**, 041 (2009)
- [24] W. Beenakker, S. Brensing, M. Kramer, A. Kulesza, E. Laenen, I. Niessen, JHEP **1008**, 098 (2010)
- [25] W. Beenakker, S. Brensing, M. Kramer, A. Kulesza, E. Laenen et al., Int. J. Mod. Phys. **A26**, 2637 (2011)
- [26] ATLAS Collab., ATLAS-CONF-2011-116 (2011)
- [27] ATLAS Collab., Eur. Phys. J. C **71**, 1630 (2011)
- [28] A.L. Read, J. Phys. G **28**, 2693 (2002)